A PRELIMINARY HYDROFOIL DESIGN INCORPORATING A CAVITATION FREE OPERATION REQUIREMENT

DECEMBER 1964

Prepared by: William D. Bauman
William D. Bauman

Approved by: T. H. Sarchin
T. H. Sarchin

Approved by: Ralph Lacey
E. R. Lacey

Technical Director: Owen H. Oakley
Owen H. Oakley

BUREAU OF SHIPS-NAVY DEPARTMENT-WASHINGTON,D.C.

AD612672

CLEARINGHOUSE FOR FEDERAL SCIENTIFIC AND TECHNICAL INFORMATION, CFSTI
INPUT SECTION 410.11

LIMITATIONS IN REPRODUCTION QUALITY OF TECHNICAL ABSTRACT BULLETIN DOCUMENTS, DEFENSE DOCUMENTATION CENTER (DDC)

☐ 1. AVAILABLE ONLY FOR REFERENCE USE AT DDC FIELD SERVICES. COPY IS NOT AVAILABLE FOR PUBLIC SALE.

☒ 2. AVAILABLE COPY WILL NOT PERMIT FULLY LEGIBLE REPRODUCTION. REPRODUCTION WILL BE MADE IF REQUESTED BY USERS OF DDC.

☒ A. COPY IS AVAILABLE FOR PUBLIC SALE.

☐ B. COPY IS NOT AVAILABLE FOR PUBLIC SALE.

☐ 3. LIMITED NUMBER OF COPIES CONTAINING COLOR OTHER THAN BLACK AND WHITE ARE AVAILABLE UNTIL STOCK IS EXHAUSTED. REPRODUCTIONS WILL BE MADE IN BLACK AND WHITE ONLY.

TSL-121-2/64

DATE PROCESSED: 3-30-65

PROCESSOR: B. Lee

DEPARTMENT OF THE NAVY
BUREAU OF SHIPS
WASHINGTON 25, D. C.

IN REPLY REFER TO
9020
Ser 420-54

16 MAR 1965

From: Chief, Bureau of Ships (Code 420)
To: Distribution List (see next page)

Subj: Transmittal of Enclosure (1)

Encl: (1) A Preliminary Hydrofoil Design Incorporating a Cavitation Free Operation Requirement

1. By this letter enclosure (1) is transmitted to the distribution list. Enclosure (1) is unclassified.

2. Enclosure (1) is incomplete in that it lacks two more appendicies and model test data, both of which are in preparation. As the additional information becomes available, it is intended to review and update enclosure (1).

Owen H. Oakley

OWEN H. OAKLEY
By direction

A PRELIMINARY HYDROFOIL DESIGN INCORPORATING A CAVITATION FREE OPERATION REQUIREMENT

DECEMBER 1964

Prepared By: William D. Bauman
WILLIAM D. BAUMAN

BLANK PAGE

Introduction

Over the past several years as the state of the art in hydrofoil design has progressed, the problem of cavitation avoidance has never been presented as part of the requirements to be satisfied in the preliminary design cycle. Cavitation becomes a problem when it develops in either of two forms 1) bubble cavitation which is associated with surface erosion and 2) sheet cavitation which is associated with a loss in lift. Prolonged bubble cavitation introduces stress concentrations and structural loss. Unexpected sheet cavitation may develop into a disasterous dynamic response. The Bureau of Ships has a continuing program to develop a design procedure, incorporating the avoidance of cavitation, and make it available to the hydrofoil designer. The procedure, some of its history and limitations is the basis of this technical memorandum.

History

This cavitation prediction technique was developed after photographs of model tests indicated that partial cavitation would be a problem on at least one hydrofoil-strut array. As the original model test program was not specifically directed toward establishing the cavitation range, a supplementary program was inagurated to fill in data points. Glass beads along the top leading edge of the hydrofoil model were suspected as being sufficient turbulence stimulators as to prematurely start cavitation. Model test flow observations with and without the glass beads verified the suspicion. The supplementary data

was then collected with a clean model. With model test data in hand, a cavitation prediction technique was developed. The prediction technique was patched together from various sources and as such is not a "closed" solution. The details are discussed in Appendix A.

To verify the prediction technique a set of hydrofoils were designed for a proposed hydrofoil ship. The preliminary design procedure for the hydrofoils with primary consideration given to avoiding cavitation is discussed in the main text. Model test correlation with theory and the details of some parametric variation studys are to be covered in Appendices now in preparation. As the correlations are established the memorandum will be revised.

Design Procedure

1. The hydrofoil design time was somewhat shortened by the restrictions imposed by the ship arrangements. A single gas-turbine engine had been selected as the power plant. Considerations of power transmission paths and air inlet paths prompted the selection of the propeller(s) aft. A canard configuration is associated with two power nacelles aft and retraction of the forward foil through the stem. A conventional configuration is associated with a single power nacelle aft and retraction of the forward foils in a transverse plane over the gunwales. After due consideration to weight distributions and arrangements the following conventional configuration was presented for a foil design:

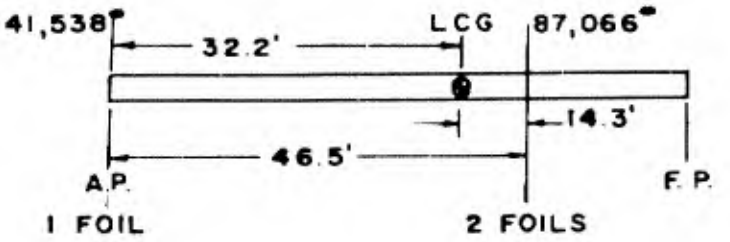

DIAGRAM I.

2. One of the first numbers to be found prior to investigating the cavitation range is the mean depth at which the foils will operate. A mean depth of 4 ft. with a keel to foil distance of 7½ ft. was calculated from considerations of structure and crew response to Sea State induced accelerations, Appendix A.

3. With an assumed foil loading (L/S) of 1250 psf which means the $\bar{C}_L$ = .175 and assuming a taper ratio $\lambda = c_T / c_R$ = .3 we calculate the center of the two-dimensional cavitation range as $\bar{C}_j$ = .1895, Appendix A. Since the ship must operate cavitation free at 50 kts, we enter Figure A2, consider the relative effects of sweep and conclude an NACA 16-(.3175).094 section swept 30° would satisfy the avoidance of cavitation requirement. The addition of the large power nacelle aft will require a thinner hydrofoil section such that the net flow velocity, locally, over the hydrofoil will not be sufficient to cause cavitation. Following the details of Appendix A we determine the section to be used as an NACA 16-(.3175).08 section.

4. If we assume the worst structural problem will arise from compressive fatigue at the maximum chord thickness at the foil nacelle junction we may construct a nomograph showing the interrelationships of foil loading, lift/drag ratio, stress and aspect ratio for a given taper ratio, velocity, sweep angle, depth and load, Appendix B. All of the latter have been determined. The nomograph indicates an aspect ratio of 6.6 will not exceed the structural requirements.

5. We have now established the aft foil conceptaully as in Figure 1. The details and assumptions may be reappraised for improvement and refinement. At the present time the case for flaps vs. incidence control has not yet been resolved. Until such time as that problem is settled the conceptual design of the forward foil is incomplete.

Conclusions

No conclusions have been made throughout this memorandum, pending model test results. After the tests of the aft foil, designated BuShips Model E, the data will be correlated with the prediction technique and some suggestions or recommendations made.

NOTATION

a	wave induced acceleration of hydrofoil ship
AR	aspect ratio of hydrofoil
b	total span of hydrofoil
C_D	drag coefficient
C_{D_I}	induced drag coefficient
$C_{\ell_0} = C_{\ell_{\Lambda=0}}$	two-dimensional, unswept lift coefficient
$\overline{C}_\ell$	average two-dimensional lift coefficient at center of two-dimensional cavitation range
C_{ℓ_α}	two-dimensional slope of C_ℓ vs α curve
ΔC_ℓ	range of C for the excursion of wave induced angles.
C_{ℓ_Λ}	two-dimensional, swept section lift coefficient
C_L	three-dimensional lift coefficient
$\overline{C}_L$	average three-dimensional lift coefficient at center of three dimensional cavitation range
$\overline{C}_{L_\alpha}$	trapezoidal-rule, average three-dimensional slope of C_L vs α
ΔC_L	width of three-dimensional cavitation range
c_R	hydrofoil root chord length at span centerline
c_T	hydrofoil tip chord
h	mean depth of hydrofoil beneath the free surface
k	span factor: $C_{\ell_{\alpha_{max}}} / \overline{C}_{L_\alpha}$
P_∞	atmospheric pressure
P	hydrostatic head
P	vapor pressure of water
ℓ/d	length/diameter ratio of nacelle
S	total planform area of the hydrofoil, as if there were no nacelle.
t/c	thickness/chord ratio

t	time in seconds
u	local velocity
V	free stream velocity
u/V	local velocity/free stream velocity ratio
x/ℓ	non-dimensionalized distance along nacelle axis
α	angle of attack
γ	taper ratio, tip chord/root chord
Λ	sweep angle of quarter streamwise chord line
$\Lambda_{c/4}$	quarter streamwise chord line
$\Lambda_{c/2}$	half streamwise chord line
ρ	density of water
ω	frequency of wave encounter

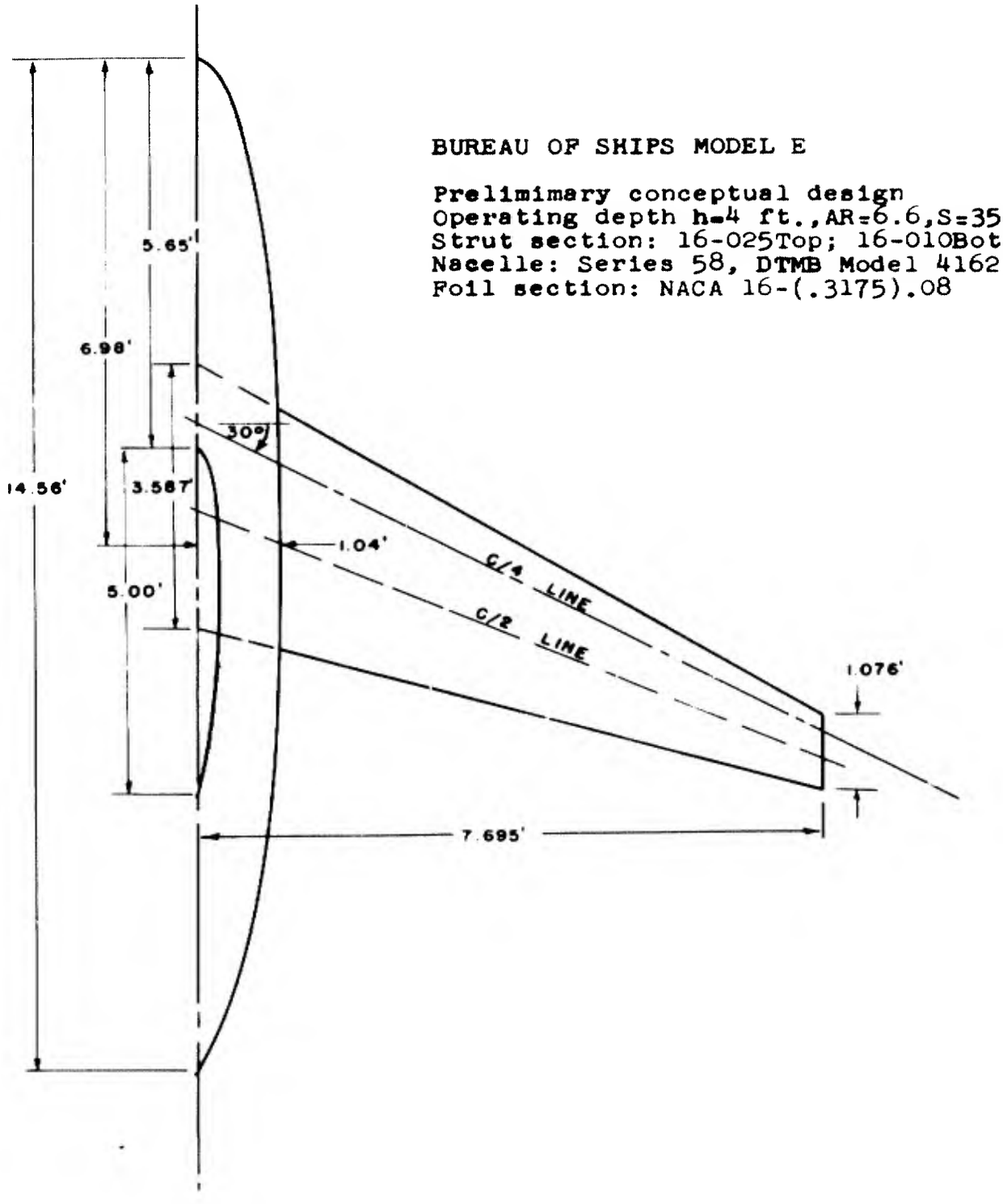

Figure 1. Preliminary conceptual design, BuShips Model E.

BLANK PAGE

APPENDIX A

In the early design stages, while studying the cavitation and seakeeping properties, two considerations must be kept in mind: (1) the foils must remain submerged while (2), the keel must clear the free surface. The subsequent compromise for these oftentimes conflicting requirements will fix the minimum length of strut and the foil submersion depth at the static flying condition. Although no rough water requirements were set in the original specifications, it was reasonable to attempt flight in Sea State 3 or 4.

Frequency of encounter for the dominant surface waves at the top of Sea State 4 with a boat speed of 50 knots into the wind is approximately 2.5 rad./sec. (Ref. A1). However, for extremes where bow slamming may occur, higher waves must also be considered. These longer waves will have longer periods which, in this case, implies that the frequency of encounter to be used should be approximately 1.5 rad. sec.

1. To examine the keel clearance let us assume the worst waves and, for convenience, take them to be sinusoidal and regular. It will be further assumed that the boat will be following some sinusoidal path, partially contouring the waves with the keel just clearing the highest waves, Diagram A1.

DIAGRAM A1.

Then the boat path is described by:

$$Z = a \sin \omega t$$

where: $2a$ = boat double amplitude (crest to trough)
ω = frequency of encounter
t = time

then $\dot{Z} = a\,\omega \cos \omega t$

and $\ddot{Z} = -a\,\omega^2 \sin \omega t$

The vertical acceleration, neglecting pitch contribution, is a maximum when $\sin \omega t = 1.0$ or

$$|\ddot{Z}| = a\,\omega^2$$

Assuming an acceptable maximum vertical acceleration of 0.25g, the allowable amplitude of motion can be determined accordingly:

$$0.25(32.2) = a\,(1.5)^2$$
$$a = 3.6 \text{ ft.}$$

Adopting a conservative viewpoint, the average of the 1/10th highest waves for the top of Sea State 4 is approximately 9 ft. double amplitude. Hence the strut length requirements can be computed to satisfy a dry keel:

1.0'	min. foil draft
+ 9.0'	double amplitude corresponding to 1/10 highest waves.
10.0'	strut length for "pure" platforming.
- 7.2'	double amplitude motion for a 0.25g allowable vert. acceleration
2.8'	available length required for strut.

On the other hand, for the significant encounter frequency of 2.5 rad./sec. (0.4 cps) corresponding to Sea State 4 conditions and 50 knot speed, the unpleasant acceleration level occurs at 0.07g, (Ref. A2). The amplitude of motion is calculated as:

$$0.07(32.2) = a\,(2.5)^2$$
$$a = 0.277 \text{ ft.}$$

and the required strut length is computed:

1.0'	min. foil draft
+ 7.0'	double amplitude corresponding to significant waves
8.0'	strut length for pure platforming
- 0.5'	double amplitude motion for 0.07g vert. acceleration
7.5'	available length required for strut

The significant wave height for Sea State 4 is approximately 7 ft. double amplitude. Hence, if a 7½ foot strut (keel to foil) is used, the ship will have platforming capabilities, based on the foil at a mean flight path of 4 ft., without encountering wave slap on the keel at Sea State 3 conditions while keeping within tolerable crew acceleration limits up through the more extreme Sea State 4 conditions.

2. The minimum range of the cavitation bucket needed for control in a fully risen sea is investigated next. For a foil of any reasonable sweep ($10° < \Lambda < 35°$) or thickness ($.06 < t/c < .10$) at 4 ft. depth, the range of the two-dimensional cavitation bucket for the excursion of wave induced angles is a ΔC_ℓ of approximately 0.160, which can be seen by plotting cavitation limits over the two extremes. In determining the width of a three-dimensional cavitation bucket from two-dimensional data, it has been shown (Ref. A3) that the Brockett method of calculating the chord-wise pressure distribution (Ref. A4) is preferable to the Abbott method. However, the Abbott method has had better correlation with experiment in predicting the top of the cavitation bucket (Ref. A3)

Before investigating the range of the cavitation bucket, some clarification should be given toward determining the cavitation bucket for a swept foil flying at the desired depth below the free surface from the Brockett program. The Brockett program was written for two-dimensional, unswept hydrofoil in an unbounded fluid. Using this to determine the two-dimensional bucket, we will next consider the three-dimensional effects. The program output lists the section lift coefficient, C_ℓ, the maximum velocity ratio $(u/v)_{max}$, and the latter's chordwise location, x/c. Cavitation inception speed at a specified depth is determined by:

$$V_k = \sqrt{\frac{P_\infty + P_h - P_v}{-\frac{1}{2}\left|1-(u/v)^2\right|\rho}}$$

where P_h is the hydrostatic head to account for the depth. To allow for sweep we use the relations:

$$V_{k_\Lambda} = V_{k_{\Lambda=0}}/\cos\Lambda \qquad \text{and} \qquad C_{\ell_\Lambda} = C_{\ell_{\Lambda=0}}\cos^2\Lambda$$

Table A1 is a suggested format to keep the calculations in an orderly scheme. A portion of an Abbott two-dimensional cavitation bucket for a swept section is shown in Figure A4.

3. We now seek a section camber to give the desired C_{ℓ_D}, such that after the three-dimensional corrections have been made to the two-dimensional Brockett bucket, the range of the three-dimensional bucket will be centered on the known operating lift coefficient $\bar{C}_L$. The effects of spanwise variation in local lift

coefficient, C_ℓ , for a swept foil with taper is plotted in Diagram A2 to illustrate a typical variation of C_ℓ or C_{ℓ_α} versus the nondimensional semispan.

Since the lift coefficient is linearly proportional to angle of attack, we can use the slope of the lift coefficient versus angle of attack, C_{ℓ_α} , in the discussion. When the hydrofoil is operating at a positive angle of attack, the maximum local lift coefficient (at approximately 3/4 semispan is related to the average lift coefficient by the ratio:

$$\overline{C}_{\ell_\alpha} = \frac{1}{S/2} \sum_{n=1}^{7} C_{\ell_\alpha} \frac{b/2}{7} c_n$$

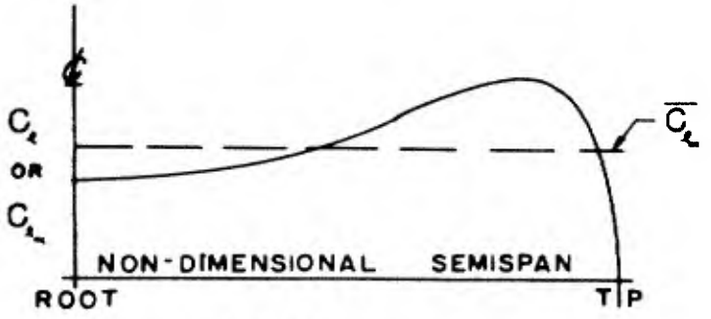

DIAGRAM A2.

$$\text{span factor} = k = \left| C_{\ell_\alpha\ max} \right| / \left| \overline{C}_{\ell_\alpha} \right|$$

The effect of planform on the two-dimensional Brockett bucket is to essentially reduce the range by k.

The span factor k is primarily a function of taper ratio for a given depth (area, aspect ratio and sweep provide a small contribution, however, and can be ignored in the first cut). The span factor k plotted against taper ratio is shown in Figure A1. The cross-hatched area represents the scatter attributable to the small contributions discussed above. Figure A2 gives the two-dimensional C_ℓ at the center of the cavitation bucket (by Brockett)

and the maximum thickness of the section to avoid 60% chord cavitation for various sweep angles $\Lambda_{c/4}$ and cambers C_{ℓ_D} . The section is here defined normal to the quarter-chord sweep line.

4. At this point we can begin to look into planform details for a specific design. Let us review what design facts we have so far:

h = 4 ft. mean depth of foils
V = 50 kts cavitation free speed
L = 20.9 tons lift per fwd foil as of 5/28/64
L = 18.5 tons lift on aft foil as of 5/28/64

Assume a loading (L/S) of approximately 1250 psf based on experience. This fixes the average three-dimensional lift coefficient at:

$\overline{C}_L = 0.175$

For an assumed taper ratio of 0.3 the span factor from Figure A1 is k = 1.22. The width of the three-dimensional cavitation bucket will then be approximately:

$\Delta C_L = \Delta C_l / k = 0.160/1.22$
$\Delta C_L = 0.1311$

At the present time, the sides of the final three-dimensional cavitation bucket are obtained by correcting both sides of the two-dimensional cavitation bucket (per Brockett) by the span factor. Since the effect is largest on the positive angle-of-attack side and as a convenient preliminary approach, the total correction is assumed on that side. The relationships are shown in Diagram A3:

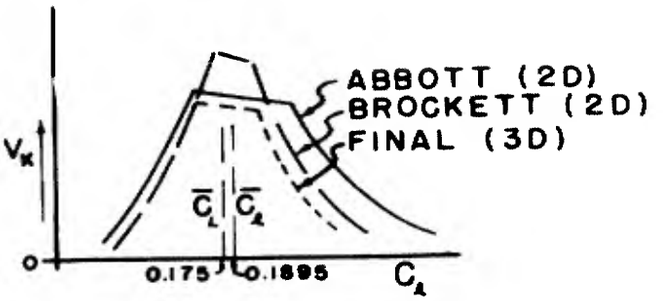

DIAGRAM A3

$\bar{C}_2$ = ½ width of Brockett bucket.
$\bar{C}_L$ = avg. 3D C_L @ center of bucket.
$\bar{C}_2$ = avg. 2D C_L @ center of bucket.

Now since only one side of the two-dimensional, swept, cavitation bucket is corrected, the center of the two-dimensional cavitation bucket, $\bar{C}_2$, is $\bar{C}_L$ plus one-half the correction.

$$\bar{C}_2 = \bar{C}_L + \left(\frac{\Delta C_L - \Delta C_L}{2}\right)$$

$$= 0.175 + \frac{(.160 - .131)}{2}$$

$$\bar{C}_2 = 0.1895$$

For an arbitrary sweep angle of 30 degrees, then C_{2_D} = 0.3175 and t/c = .094 from Figure A2. If we sweep the foil only 20 degrees then C_{2_D} = 0.277 and t/c = .0805. For a 10 degree sweep, C_{2_D} = 0.2525 and t/c = .0758. Considering the structural problem of spanwise bending, which may be discussed in another Appendix, the 30 degree sweep is most advantageous since it allows the thickest section. This we choose.

Having selected a sweep of 30 degrees, let us examine the effects of taper ratio selection. Choosing a taper ratio of 0.20, then:

$$k = 1.35$$

$$\Delta C_L = \Delta C_\ell / k$$

$$= 0.160/1.35 = 0.1185$$

$$\bar{C}_\ell = \bar{C}_L + \left(\frac{\Delta C_\ell - \Delta C_L}{2}\right)$$

$$= 0.175 + \left(\frac{0.160 - 0.1185}{2}\right) = .1957$$

$$C_{\ell_D} = 0.3275$$

$$t/c = 0.0920$$

For a taper ratio of 0.4,

$$\Delta C_L = 0.160/1.16 = 0.1379$$

$$\bar{C}_\ell = 0.175 - \left(\frac{0.160 - 0.1379}{2}\right)$$

$$C_{\ell_D} = 0.310$$

$$t/c = 0.0954$$

The above correction for three-dimensional effects with the free surface was determined theoretically for hydrofoils on the basis of no nacelles nor struts. Limited experimental data (Ref. A3) indicates that an additional correction should be made to account for the nacelle and strut. The available data was for a taper ratio of 0.3 which motivated the choice for λ = 0.4 or 0.2. Further model tests will be necessary to better define the span factor.

5. Before going further into the design it is well to point out one limitation introduced when using Figure A2. The foil thickness to avoid 60% chord cavitation limits was determined

on the basis of speed (i.e. the upper right hand corner of the cavitation bucket Figure A3) with no allowance made for a nacelle. If we were to assume our hydrofoil was a two-dimensional NACA 16 -(.3175) .094 section swept 30° at h = 4 ft., then in the (kink)* region we would expect cavitation limits to be defined by the streamwise NACA 16-(.2749) .081 section (0.094 cos 30° = .081). This is only valid in the two-dimensional case, where taper has no meaning. With a swept, tapered foil, the streamwise section will no longer remain a NACA 16 section. However, the approximation is necessitated by the suggestion from Ref. A6 that the lifting line going from tip to centerline on the planform should most probably curve to meet normal to the foil centerline. On the basis of that assumption, Figure A3 indicates incipient cavitation will occur at C_{ℓ} = .175 and V_k = 50 knots which is unfortunately the three-dimensional design condition. It is apparent that to circumvent the bounds on incipient cavitation at the kink region we will need a thinner section to provide the speed margin we will lose by adding a nacelle.

The present ship arrangements dictate an airplane configuration with a single power nacelle aft. This nacelle (physically large due to the right-angle drive mechanism) will be the deciding factor on cavitation speed. Let us assume a Series 58 type of nacelle, DTMB Model 4162 of length/diameter ratio 7.0. Then from a plot of u/V versus x/l (Ref. A7), the minimum velocity ratio is seen to occur at x/l = 0.48. This gives a value of (Δ u/V) nacelle = 0.0344. As a simplification, the peripheral jump in

* For swept foils, the kink region is an area of about one root chord total width at the midspan, Ref. A3 & A6.

velocity ratio due to the difference in depth over the upper and lower surface can be ignored. To obtain a minimum net velocity ratio along the foil-nacelle junction, we require the 60% chord line of the hydrofoil to intersect the nacelle surface at the nacelle station corresponding to $x/\ell = 0.48$. This restriction fixes a common point of maximum velocity on the hydrofoil section with minimum velocity on the nacelle surface. Although this choice may not be optimum, the fact remains that if we can successfully predict satisfactory cavitation limits for this case then we will gain more confidence while justifying the procedure. This will then permit us to use an established "modus operandi" to investigate other arrangements for succeeding design recycles.

To allow for the effects of viscosity and the interference flow filleting in the nacelle-foil junction which generally increases the pressure, we will assume $\Delta u/V)_{\text{nacelle}} = 0.024$ rather than 0.0344 which was for the unbounded fluid case. From experience, the foil section thickness, t/c, can be reduced from 0.094 to 0.080. The streamwise section at the kink region is then approximately a NACA 16 (.2749) 0.069 with $\Lambda_{\%} = 0.0^{\circ}$ at h = 4'. Following the method of Ref. A3, we correct the 1.25% and 60% chord perturbation velocity contributions due to angle of attack for the change in pressure pattern of Ref. A6 and for the presence of the nacelle. 6. In correcting the top of the cavitation bucket for kink and nacelle effects, since Ref. A3 omitted some of the details, more details may be in order. Using the Abbott method of obtaining

cavitation limits, the computer output, Table A3, lists the u/V) max, its chordwise location, the critical velocity and the section lift coefficient. Ref. A6 suggests the pressure distribution at the centerline due to angle of attack be altered in profile but retaining the same net contribution. To accomplish this, we must isolate out the contribution due to angle of attack from the total pressure contributions using the Abbott procedure. This contribution due to angle attack must then be modified for the kink effect and then checked for any subsequent possible shift in maximum $u/V)_{TOTAL}$ which depends on plus or minus angle of attack at top or bottom surface respectively. The perturbation velocity due to the nacelle is then thrown in and the subsequent figures recalculated to get the corrected cavitation inception speed.

For the unswept section at the design lift coefficient, all the contributions to the perturbation velocity are attributable to thickness and camber. Hence to accomplish the preceding we take the computer results, Table A3, which give:

Base No. = $(u/V)_{TOTAL}$ = 1.148 at x/c = 0.60 TOP

Since the computer does not provide the Base No. at x/c = 0.0125, we must hand calculate it. We obtain:

Base No. - $(u/V)_{TOTAL}$ = 0.9589 at x/c = 0.0125 BOT

For all angles of attack

$$\left(\frac{u}{V}\right)_{TOTAL} = \left(\frac{u}{V}\right)_t \pm \left(\frac{\Delta u}{V}\right) C_{L_D} \pm (\text{sign } \alpha) \left(\frac{\Delta u}{V}\right) f(\alpha) + \left(\frac{\Delta u}{V}\right)_{NACELLE}$$

where upper signs refer to the upper surface and lower signs refer to the lower surface u/V

Diagram A3, (a), (b), and (c) illustrates the three typical velocity profiles due to thickness, camber and angle of attack respectively. Diagram A3, (e), (f), and (g) illustrate the results of u/V additions at three angles of attack. Notice that for small negative angles Diagram A3 (f), there is very little difference in $(u/V)_{TOTAL}$ at x/c = 0.02 bottom and x/c = 0.60 top locations. After the kink correction has been made to the original $(\Delta u/V)_{\alpha}$ according to Table B1 of Ref. 3, we might expect the maximum $(u/V)_{TOTAL}$ to remain at x/c = 0.60 throughout a greater C_{ℓ} range. Table A2 provides a suggested format for tabulating the calculations in an orderly manner. Using Table A2, a comparison of the magnitudes of $(u/V)_{TOTAL}$ at the two x/c locations in Column 5, indicates the choice of the maximum $(u/V)_{TOTAL}$ at x/c = 0.60 to govern throughout the greater C_{ℓ} range. The result which includes the nacelle effect, Figure A4 is the desired cavitation limit (from columns 1 and 6) applicable to the kink region.

7. The remaining problem now is to examine the effects of wing loading and aspect ratio for the actual foil. To validate the theoretical model discussed in the preceding paragraphs on the various parameters so affecting cavitation inception, we resort to experimentation. This implies controlled model testing. To isolate the individual parameters in a model test usually conducted individually with forward and after foils, it is essential to keep the differences (aspect ratio, sweep, and other parameters) between forward and aft foils to a minimum so that a parametric study will not be too confusing.

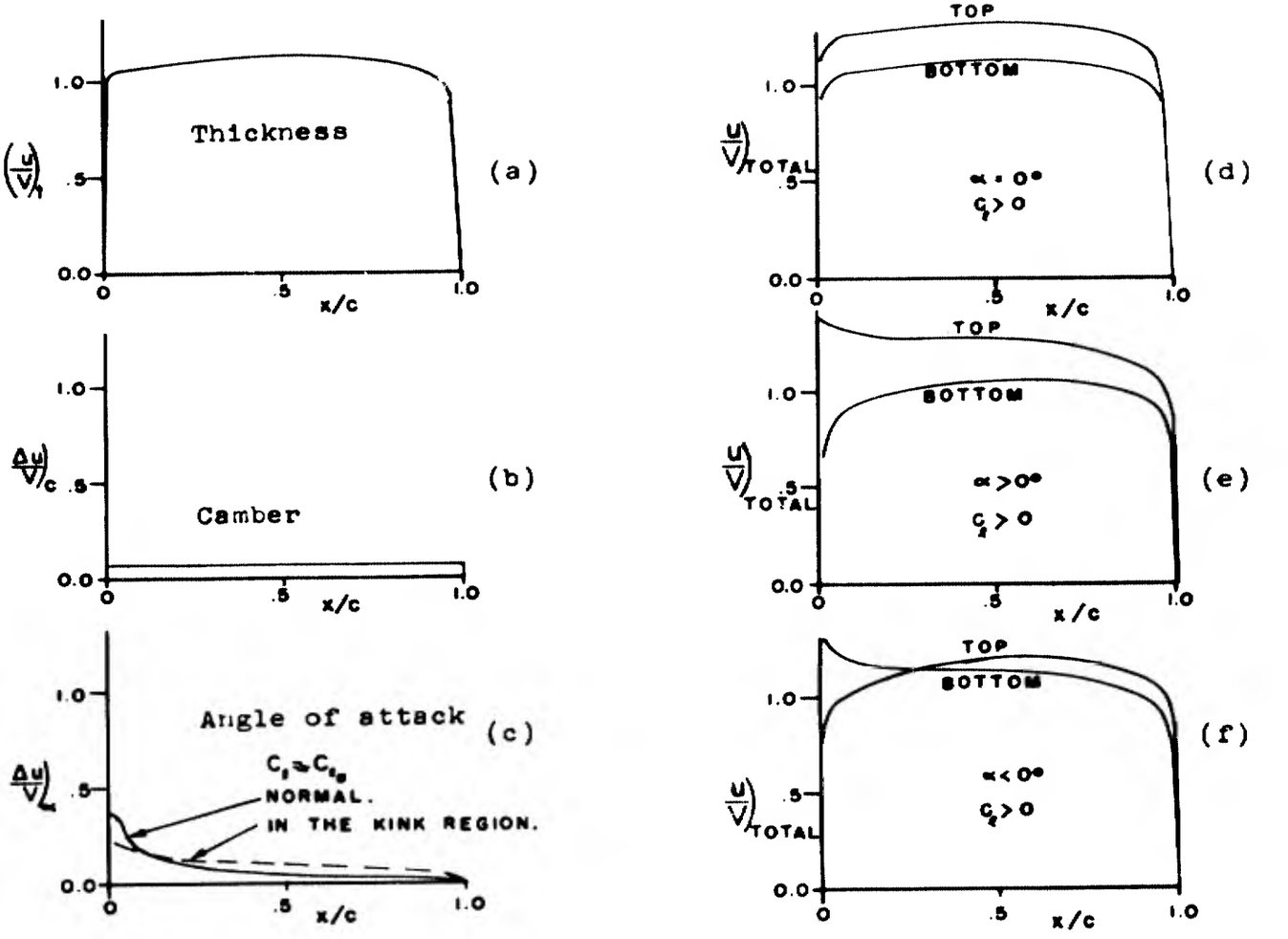

COMPONENT VELOCITY DISTRIBUTIONS

TOTAL VELOCITY DISTRIBUTIONS
(NO NACELLE NOR KINK EFFECTS)

DIAGRAM A 3 TYPICAL VELOCITY DISTRIBUTIONS.

BLANK PAGE

A common area of 35.88ϕ was chosen. For the present area distribution of the present system this implies a slight bias toward a lower foil loading on the aft foil with a correspondingly high loading on the forward foils. Low foil loadings are good from a cavitation viewpoint especially where a large nacelle is superimposed.

To illustrate the effect of loading, let us retain the same working data as used previously. We then have for the aft foil:

L = 18.5 tons	V = 50 knots
S = 35.88 ft.	C = 0.162
h = 4 ft.	η = 0.30
$\Lambda_{c/4}$ = 30.0 degrees	

Foil Section: NACA 16-(.3175) .080
Nacelle: Series 58, DTMB Model 4168, l/d = 7.0

The apparent effect of the reduced foil loading for the aft foil is to change the operating $\bar{C}_L$ from 0.175 to 0.162 as shown below:

$\bar{C}_{L_1} = L/S/(\frac{1}{2}\rho U^2) = 0.175$

$S_1 = L/(L/S_1) = (18.5)(2240)/1250$

$S_1 = 33.152$

$\bar{C}_{L_2} = \bar{C}_L (S_1/S_2) = (0.175)(33.152/35.88)$

$\bar{C}_L = 0.162$

To investigate the effect of aspect ratio, let us first assume a fatigue limit of 80 ksi. Then using a 16-X08 section, we enter the nomograph in Appendix B, Figure B1 and observe that an aspect ratio greater than 6 is needed. As a practical compromise, let us set the aspect ratio at 6.6 which will result in a lift/drag of approximately 17. In utilizing the nomograph it must be pointed out that it was based on no nacelle, with the strut chord equal

to the foil root chord and C_{D_f} = 0.0028.

The following additional data is now pertinent:

c_r = 3.587 ft. AR = 6.6
c_t = 1.076 ft.

With this additional data, we calculate the specific cavitation bounds for the aft foil as per Table B2 of Ref 3. The results can be seen in Figure A5. It is to be noted that the calculations have been carried out with the total planform area method without discounting the panel area covered by the nacelle. The exposed foil area method as discussed in Ref. 3 involves more detailed analysis and within the framework of engineering approximations did not show a noticeable improvement in comparison to experiment as can be seen in the Figures 5B and 6 of Ref. 3. On the other hand, the cavitation buckets of Ref. 3 were based on total planform area and that procedure has been followed here.

REFERENCES

(A1) Martin, M., and Turpin, F., "The Effects of Surface Waves on Some Design Parameters of a Hydrofoil Boat," Hydronautics, Inc. Technical Report 001-3

(A2) Buchmann, E., "Criteria for Human Reaction to Environmental Vibration on Naval Ships," DTMB Report 1635

(A3) Johnson, R.S., "Prediction of Lift and Cavitation Characteristics of Hydrofoil-Strut Arrays," Paper presented at the Southern California Section, SNAME, March 1964

(A4) Brockett, T., DTMB Report 1821, in preparation.

(A5) Abbott, I.H. and von Doenhoff, A.E., "Theory of Wing Sections," Dover Publications, New York 1959

(A6) Thwaites, B., "Incompressible Aerodynamics," Oxford U. Press, Great Britain, 1960

(A7) Moore, W.L., "Bodies of Revolution with High Cavitation-Inception Speeds - For Application to the Design of Hydrofoil-Boat Nacelles," DTMB Report 1669 September 1962

BLANK PAGE

STANDARD WORK SHEET
NAVSHIPS 3627 (11-67)

TABLE A-1

$C_{\ell_{\Lambda=0}}$	$\left(\frac{u}{V}\right)_{max}$	$V_{K_{incep}}$		$C_{\ell_{\Lambda=30^\circ}}$	$V_{K_{incep_{\Lambda=30^\circ}}}$
.0784	1.349	31.6		.0588	36.5
.1036	1.278	35.8		.0777	41.3
.1288	1.212	42.0		.0966	48.5
.1540	1.152	49.8		.1155	57.5
.1792	1.140	52.2		.1344	60.3
.2044	1.143	51.2		.1533	59.5
.2297	1.146	51.0		.1723	58.9
.2549	1.149	50.3		.1912	58.1
.2801	1.152	49.8		.2101	57.5
.3054	1.155	49.3		.2290	56.9
.3306	1.174	46.6		.2480	53.8
.3558	1.204	42.7		.2669	49.3
.3810	1.240	39.1		.2858	45.1
.4062	1.285	35.4		.3047	40.9
.4315	1.336	32.3		.3236	37.3
.4567	1.394	29.4		.3425	33.9
			$C_{\ell_{\Lambda=30^\circ}} = C_{\ell_{\Lambda=0}} \cos^2\Lambda$		
			$V_{K_{\Lambda=30^\circ}} = V_{K_{\Lambda=0}} / \cos^2\Lambda$		

Determination of cavitation inception limits for NACA 16-(.3175).08 Section at h = 4 and $\Lambda = 30^\circ$ from Brockett program computer output.

STANDARD WORK SHEET
NAVSHIPS 3523 (11-67)

TABLE A-2

① C_l	② x/c	③ $\frac{\Delta v_a}{V}$	④ $\frac{\Delta v_i}{V}\left[\frac{\left(\frac{\Delta v}{V}\right)_{kink}}{\left(\frac{\Delta v}{V}\right)_{2D}}\right]$	⑤ $\left(\frac{u}{V}\right)_{TOTAL\ with\ nacelle}$	⑥ $V_{K_{INCEP}}$	⑦ $\frac{x}{c}$
-.0001	.0125 / 60	+.3153 / -.0354	.1501 / -.0560	1.1332 / 1.1160	53.6	.0125
+.0499	.0125 / .60	+.3071 / -.0293	.1228 / -.0457	1.1051 / 1.1264	55.1	.60
.0999	.0125 / .60	+.2364 / -.0228	.0955 / -.0355	1.0784 / 1.1366	53.0	.60
.1499	.60	-.0163	-.0254	1.1467	51.0	.60
.1999	.60	-.0098	-.0153	1.1568	49.3	.60
.2499	.60	-.0033	-.0051	1.1670	47.7	.60
.2999	.60	+.0032	+.0050	1.1771	46.1	.60
Base No.	at x/c =	60% is	1.1481	for +α		
Base No.	at x/c =	1.25% is	0.9589	for +α		
$\left(\frac{\Delta v_a}{V}\right)_{kink}$	= 1.56	at x/c = 60%				
$\left(\frac{\Delta v_i}{V}\right)_{2D}$	= 0.40	at x/c = 1.25%				
$\frac{\Delta v}{V}$ nacelle	= .024					

Determination of cavitation inception limits in kink region with nacelle contribution.

TABLE A-3

FROM RSJ 080 AS OF 8/ 2/64
NACA 16 SERIES, WITH AN A = 1.0 MEAN LINE
SWEEP = 0.00 DEG
IDEAL CL2D = .27480 THICKNESS = .06900
CRIT. SPEED(KTS) AT 4.000 FEET

SURFACE	X/C	(U/V)TOT	U(CRIT)	CL2D
BOTTOM	0.00	1.4514	27.20	-.0251
BOTTOM	1.25	1.3342	32.40	-.0001
BOTTOM	1.25	1.3001	34.45	.0249
BOTTOM	1.25	1.2660	36.86	.0499
BOTTOM	1.25	1.2319	39.78	.0749
BOTTOM	1.25	1.1978	43.40	.0999
BOTTOM	1.25	1.1637	48.09	.1249
TOP	60.00	1.1318	53.08	.1499
TOP	60.00	1.1359	52.76	.1749
TOP	60.00	1.1383	52.62	.1999
TOP	60.00	1.1415	51.97	.2249
TOP	60.00	1.1448	51.34	.2499
TOP	60.00	1.1481	50.74	.2749
TOP	60.00	1.1513	50.15	.2999
TOP	1.25	1.1647	47.92	.3249
TOP	1.25	1.1988	43.29	.3499
TOP	1.25	1.2329	39.68	.3749
TOP	1.25	1.2670	36.78	.3999
TOP	1.25	1.3011	34.38	.4249
TOP	1.25	1.3352	32.34	.4499
TOP	1.25	1.3693	30.50	.4749
TOP	1.25	1.4034	29.06	.4999
TOP	1.25	1.4375	27.71	.5249
TOP	1.25	1.4716	26.50	.5499
TOP	1.25	1.5057	25.42	.5749

Computer output of cavitation inception calculation by Abbott method.

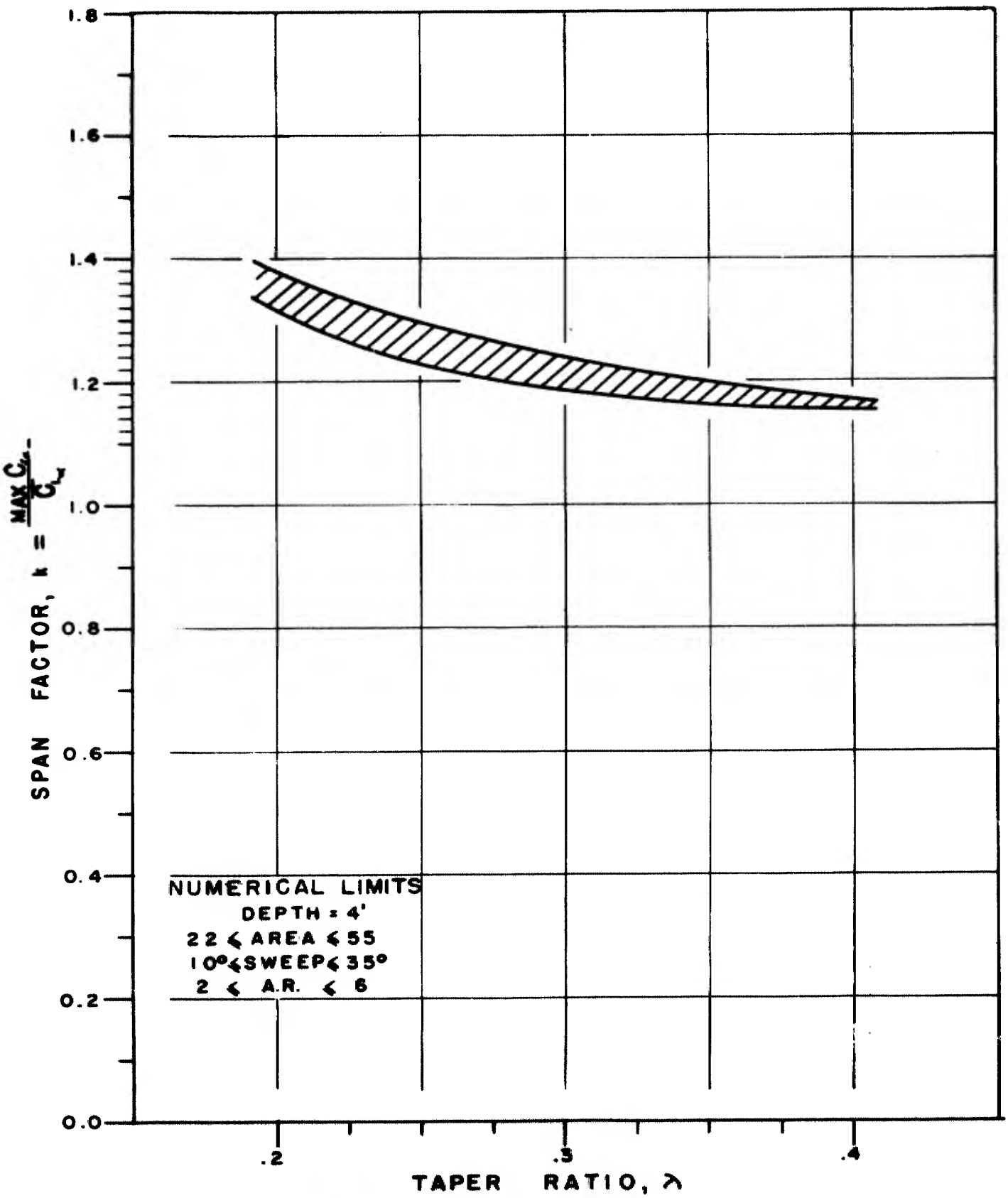

FIGURE A1. SPAN FACTOR VS. TAPER RATIO.

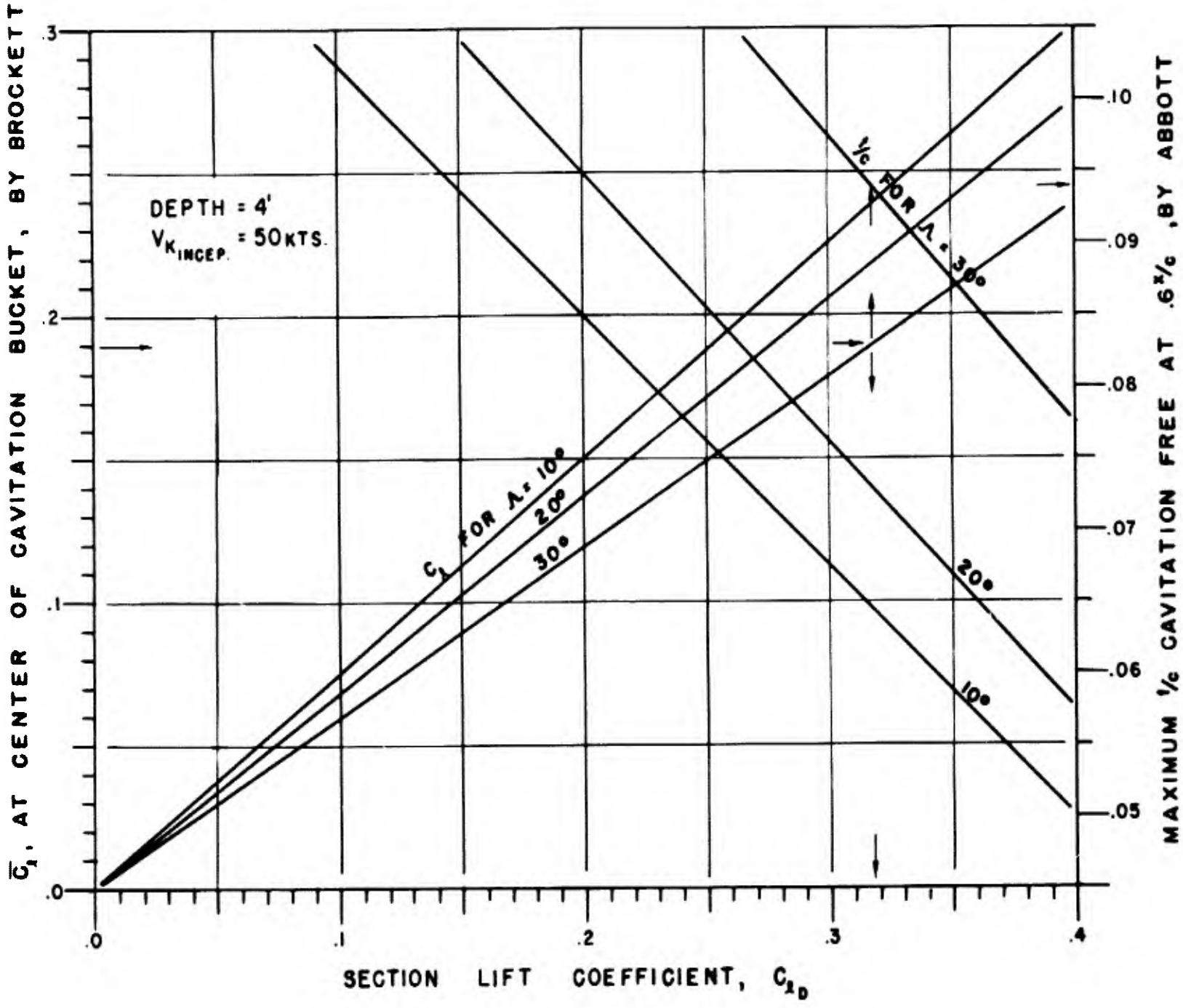
DEPTH = 4'
$V_{K_{INCEP.}}$ = 50KTS.
C_l FOR Λ = 10°
20°
30°
1/c FOR Λ = 30°
20°
10°
$\overline{C_l}$, AT CENTER OF CAVITATION BUCKET, BY BROCKETT
MAXIMUM 1/c CAVITATION FREE AT .6 1/c, BY ABBOTT
SECTION LIFT COEFFICIENT, C_{l_D}
.0
.1
.2
.3
.4
.05
.06
.07
.08
.09
.10

FIGURE A2.

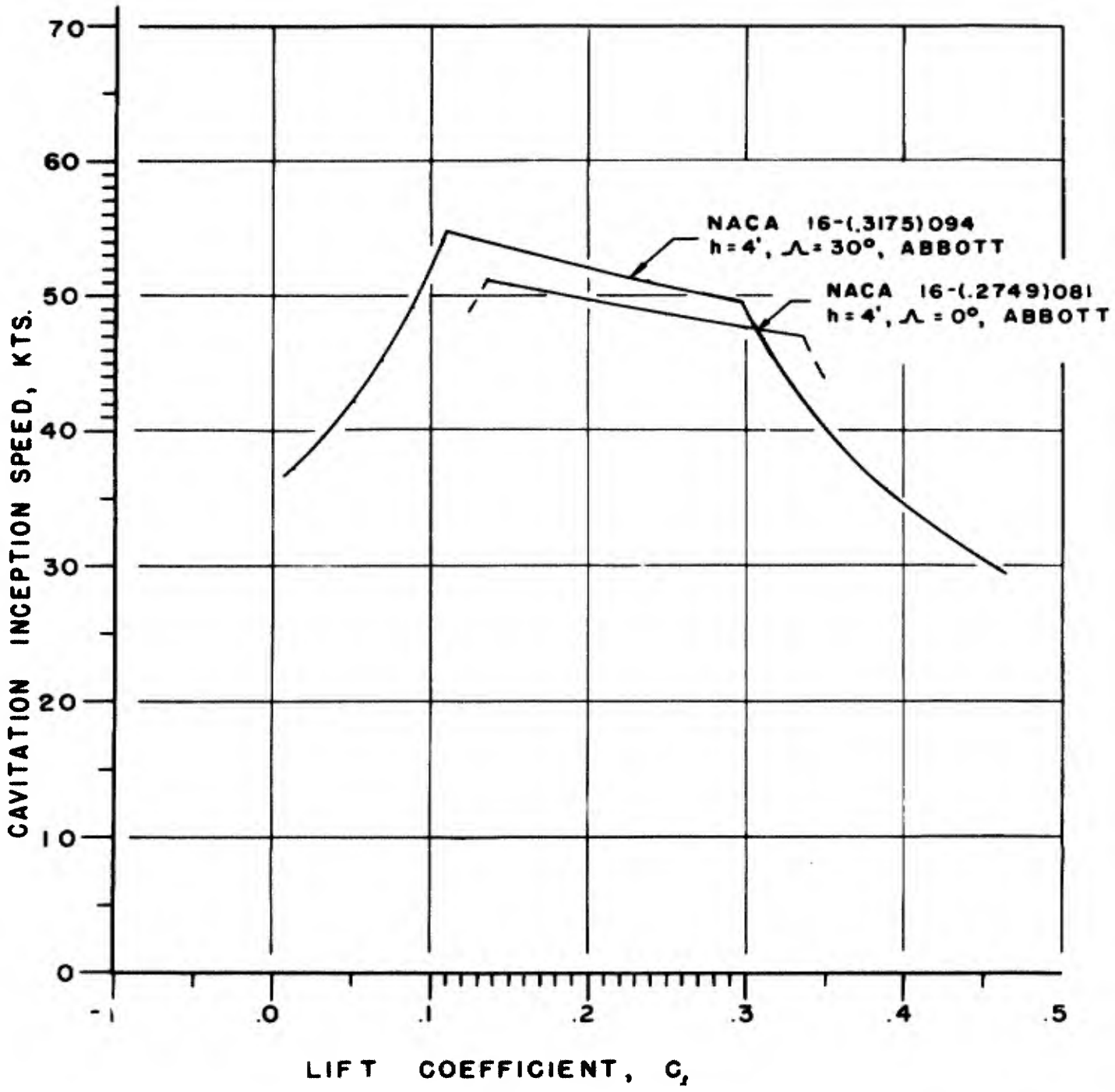

FIGURE A3. CAVITATION LIMITS, 2-DIMENSIONAL.

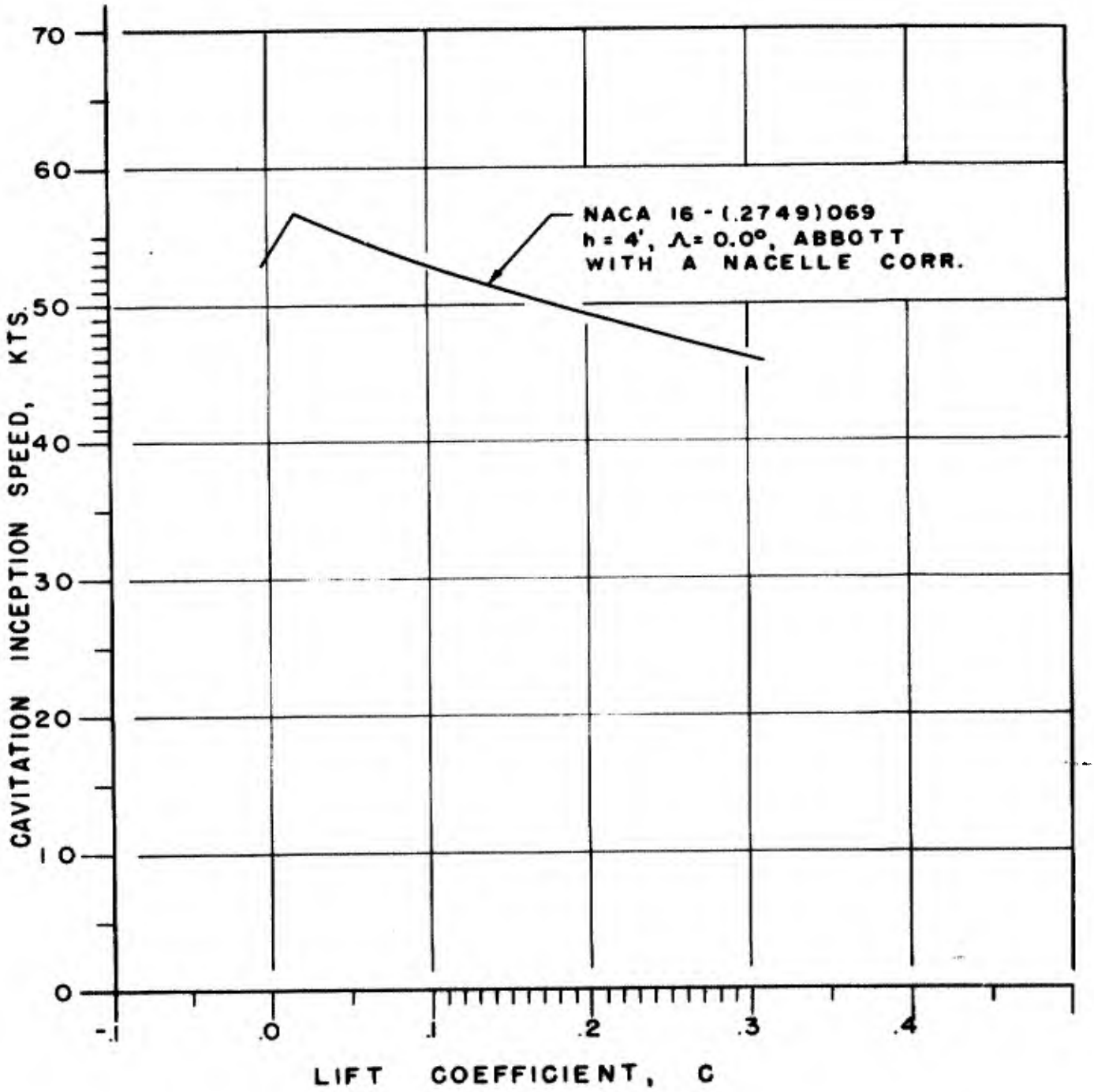

FIGURE A4. CAVITATION LIMITS, KINKED REGION WITH POD.

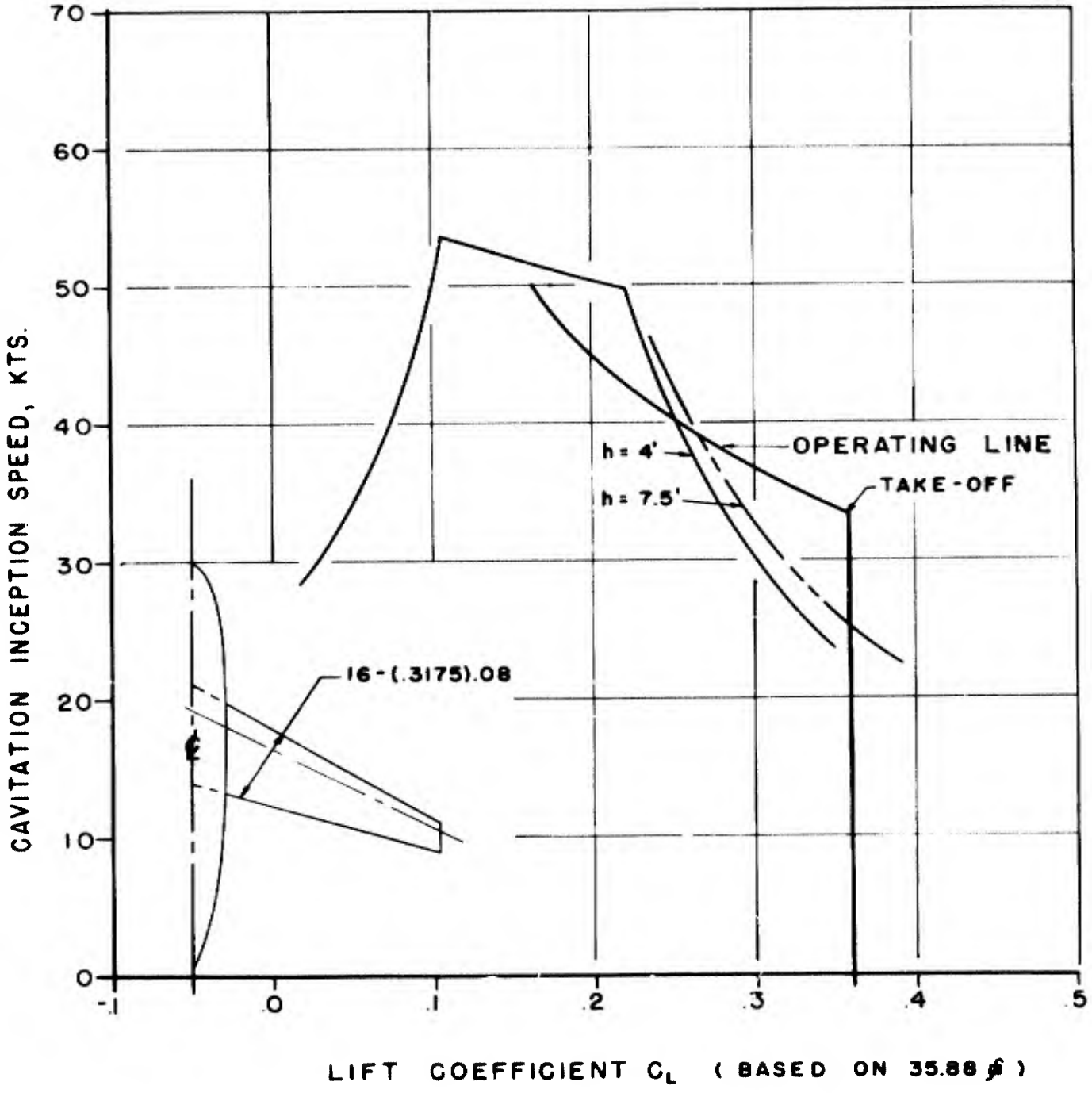

FIGURE A5. THREE DIMENSIONAL CAVITATION LIMITS.

DISTRIBUTION LIST

Chief, Bureau of Ships (20)
Navy Department
Washington, D. C. 20360
Attn: Code 210L (3)
Code 345 (1)
Code 420 (12)
Code 442 (1)
Code 449 (1)
Code 632 (1)
Code 341B (1)

Commanding Officer and Director
David Taylor Model Basin (10)
Carderock, Maryland
Attn: Code 500 (1)
Code 513 (1)
Code 520 (1)
Code 526 (1)
Code 530 (1)
Code 580 (1)
Code 589 (1)
Code 142 (2)
Code 525 (1)

David Taylor Model Basin (1)
High Speed Phenomena Division
Langley Field, Virginia
Attn: Mr. R. E. Olsen

Chief, Office of Naval Research (2)
Navy Department
Washington 25, D. C.
Attn: Code 438

Chief, Bureau of Naval Weapons (2)
Navy Department
Washington 25, D. C.
Attn: Code RAAD-334 (1)
Code RRSY-1 (1)

Langley Aeronautical Laboratory (1)
National Aeronautics and Space Administration
Langley Air Force Base
Langley Field, Virginia

Chief of Naval Operations (1)
Navy Department
Washington 25, D. C.
Attn: LCDR W. Norris (Cp-725)

DISTRIBUTION LIST

Scientific and Technical Information Facility (2)
Attn: NASA Representative (SAK/DL-50h)
P. O. Box 5700
Bethesda, Maryland

State University of Iowa (1)
Iowa Institute of Hydraulic Research
Iowa City, Iowa

Southwest Research Institute (1)
8500 Culebra Road
San Antonio 6, Texas
Attn: H. N. Abramson, Director of Mechanical Science

Oceanics, Inc., (1)
114 East 40 Street
New York 16, New York
Attn: Dr. Paul Kaplan

Stanford University (1)
Stanford, California
Attn: Head, Civil Engineering

Boeing Airplane Company (1)
Aero-Space Division
Box 3707
Seattle, Washington

California Institute of Technology (1)
Pasadena, California
Attn Hydrodynamics Laboratory

Director, Stevens Institute of Technology (1)
Davidson Laboratory
Castle Point Station
Hoboken, New Jersey

Hydronautics, Incorporated (1)
Pindell School Road
Howard County
Laurel, Maryland

Massachusetts Institute of Technology (1)
Department of Naval Architecture and Marine Engineering
Cambridge 39, Massachusetts

DISTRIBUTION LIST

St. Anthony Falls Hydraulic Laboratory (1)
University of Minnesota
Hennepin Island,
Minneapolis 14, Minnesota

Technical Research Group, Inc. (1)
Route 110
Melville, New York

Aerojet General Corporation (1)
Azusa, California
Attn: Mr. J. Levy

U. S. Navy Ordnance Test Station (1)
Oceanic Research Group
3202 E. Foothill Blvd.
Pasadena, California

Lockheed Aircraft Corporation (1)
Hydrodynamic Group
Sunnyvale, California
Attn: Mr. R. [illegible]

Grumman Aircraft Engineering Corporation (1)
Marine Engineering Section
Bethpage, Long Island, New York

University of California (1)
Institute of Engineering Research
Berkeley, California
Attn: Professor R. Paulling

General Dynamics/ Convair (1)
P. O. Box 1950
San Diego 12, California
Attn: Mr. R. Oversmith

Defense Documentation Center (20)
Cameron Station
Alexandria, Va.

Revised 12/10/63